MIT Open Access Articles

On the effect of surface roughness height, wettability, and nanoporosity on Leidenfrost phenomena

Massachusetts Institute of Technology

DSpace@MIT

On the effect of surface roughness height, wettability, and nanoporosity on Leidenfrost phenomena

Hyungdae Kim,[1,2] Bao Truong,[1] Jacopo Buongiorno,[1,a] and Lin-Wen Hu[3]

[1]*Department of Nuclear Science and Engineering, Massachusetts Institute of Technology, Cambridge, Massachusetts 02139, USA*
[2]*Department of Nuclear Engineering, Kyung Hee University, Youngin, Gyeonggi 446-701, South Korea*
[3]*Nuclear Reactor Laboratory, Massachusetts Institute of Technology, Cambridge, Massachusetts 02139, USA*

In recent quenching heat transfer studies of nanofluids, it was found that deposition of nanoparticles on a surface raises its Leidenfrost point (LFP) considerably [Kim *et al.*, Int. J. Multiphase Flow **35**, 427 (2009) and Kim *et al.*, Int. J. Heat Mass Transfer **53**, 1542 (2010)]. To probe the physical mechanism underlying this observation, the effects of surface properties on LFP of water droplets were studied, using custom-fabricated surfaces for which roughness height, wettability, and porosity were controlled at the nanoscale. This approach reveals that nanoporosity is the crucial feature in efficiently increasing the LFP by initiating heterogeneous nucleation of bubbles during short-lived solid-liquid contacts, which results in disruption of the vapor film. © *2011 American Institute of Physics*. [doi:10.1063/1.3560060]

When a liquid droplet is placed on a surface held at a temperature much higher than the liquid's boiling point, it hovers on a vapor cushion without wetting the surface. This phenomenon is called film boiling and occurs at surface temperatures beyond the so-called "*Leidenfrost point (LFP)*." If the surface temperature is at or above the LFP, heat transfer from the surface to the liquid takes place by conduction and radiation through the vapor layer, and thus the liquid takes a significantly longer time to evaporate than it would on a surface held at lower temperature. Therefore, higher LFP is desirable for rapid cooling of overheated components in high-power-density thermal systems, such as nuclear reactors during hypothetical accidents.

In recent film boiling heat transfer studies with nanofluids, we demonstrated that deposition of nanoparticles on a surface significantly increases the nominal LFP up to ~500 °C under atmospheric and saturated conditions, considerably accelerating the transient cooling of overheated objects.[1,2] However, such a high LFP could not be explained by the traditional LFP models based on hydrodynamic instability of the vapor film, e.g., Berenson's[3] and Henry's[4] models. This suggested that the vapor film is destabilized and disrupted by a different mechanism associated with the thin nanoparticle deposition layer. Characterization of the deposition layer suggested changes in roughness, wettability, and nanoscale porosity as plausible causes for such a high LFP. Nevertheless, it was not possible to identify the exact physical mechanism of LFP enhancement because nanoparticle deposition in those experiments changed roughness height, wettability, and porosity simultaneously. Therefore, we decided to investigate LFP phenomena with custom-fabricated surfaces for which we can precisely separate the effects of roughness height, wettability, and nanoporosity, as explained next.

Surface roughness height was controlled by fabricating cylindrical posts of 15 μm height and 5 μm diameter on a

nanosmooth silicon wafer ($R_a < 0.5$ nm; thickness 380 μm) [Fig. 1(b)]. The posts were fabricated with a deep reactive-ion etching process, and were arranged on a square array of large pitch (500 μm), to prevent secondary effects, such as capillarity. Next, the surface intrinsic wettability was controlled by depositing a nanosmooth thin layer of gold (100 nm thick) or silicon oxide (20 nm thick) with a sputtering technique; the resulting contact angles for de-ionized water droplets were found to be 83° on the gold surface and 19° on the silicon oxide surface (see the insets of Fig. 1). Note that the presence of the microposts does not affect wettability [compare insets of Figs. 1(a) and 1(b)], which was expected, given the large pitch of the post array. Finally, to explore the effect of nanoporosity, we used a thin nanoporous layer (about 600 nm thick) made of silicon oxide nanoparticles (23 nm), deposited according to the layer-by-layer (LBL) process
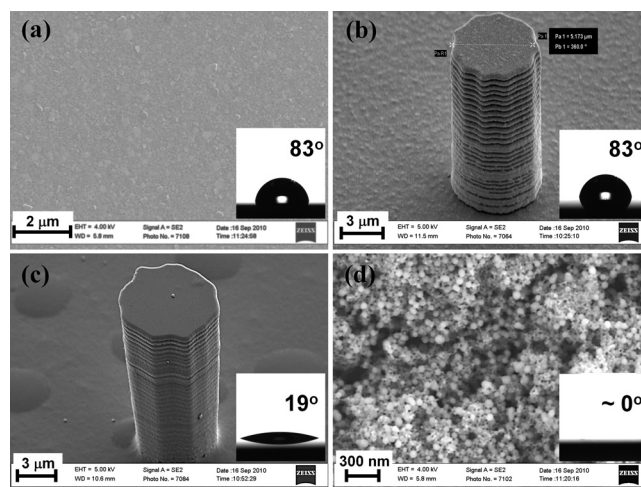

FIG. 1. SEM images of fabricated samples for LFP tests: (a) smooth Au layer; (b) 15 μm posts on smooth Au layer; (c) 15 μm posts on smooth SiO$_2$ layer; (d) LBL SiO$_2$ layer. Insets show static equilibrium contact angle on the fabricated samples for 10 μL water droplets on (a) smooth Au (83°), (b) Au with microposts (83°), (c) SiO$_2$ layer (19°), and (d) nanoporous SiO$_2$ layer (~0°).

[a]Author to whom correspondence should be addressed. Electronic mail: jacopo@mit.edu. Tel.: +1-617-253-7316.
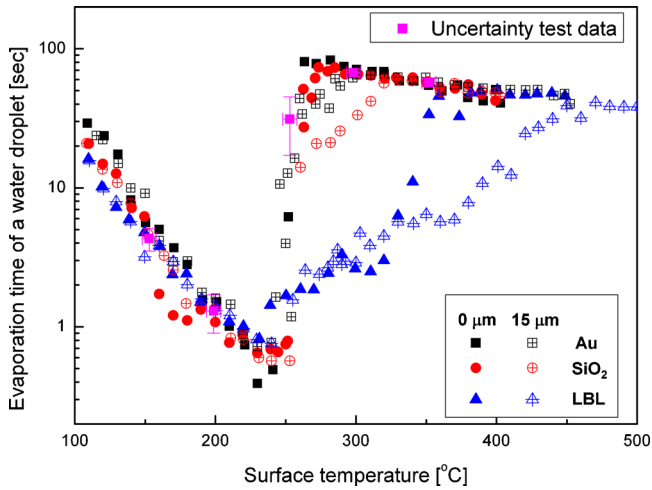
98, 083121-1

FIG. 2. (Color online) Water droplet evaporation time vs surface temperature. The error bars attached to the filled pink diamond symbols represent the standard deviation of nominally identical tests on the smooth Au-coated surface. The nominal uncertainty in the measurement of the LFP temperature was found to be less than ±5 °C.

TABLE I. Summary of LFP temperatures for water on the test surfaces (°C).

Micropost height (μm)	Au	SiO$_2$	Nanoporous SiO$_2$
0	264 ± 5	274 ± 5	359 ± 5
15	290 ± 5	325 ± 5	453 ± 5

described by Lee *et al.*[5] The nanoporous layer causes a further enhancement in the apparent wettability [the contact angle decreases to ∼0°, as shown in Fig. 1(d)] with respect to the smooth silicon oxide surface (19°). This is due to the well-known Wenzel effect.[6] On the other hand, the roughness height change due to the nanoporous layer is negligible (≤ 0.016 μm). In summary, using a combination of spaced-out microposts, and smooth and nanoporous layers we were able to control surface roughness height, wettability, and nanoporosity independently.

A common technique used for determining the LFP consists in measuring the evaporation times of liquid droplets over a heated surface. The test surface is sandwiched between two independently heated and controlled copper blocks. The upper block has a through-hole in the shape of an inverted cone to place a droplet on the silicon wafer and keep the evaporating droplet on the silicon wafer. The temperature difference between the two blocks was controlled to be less than 1 K during the experiments. A water droplet of ∼2.9 mm in diameter is released on the test surface from a height of 1.5 mm using a syringe, and the evaporation time is measured with a stopwatch. The uncertainty in the evaporation time measurement was found to be ∼0.4 s from a set of tests at representative conditions.

The data obtained from the droplet experiments are displayed as droplet evaporation time versus surface temperature in Fig. 2. In this curve, the temperature corresponding to the longest evaporation time is the LFP. The LFP on the smooth gold surface without microposts is ∼264 °C, reasonably closed to the values found in the literature.[7] The LFP is slightly higher (∼274 °C) for the smooth silicon oxide surface without microposts but is significantly higher (∼359 °C) for the porous silicon oxide surface without microposts. This result suggests that nanoporosity has a stronger effect than intrinsic surface wettability on the LFP. The effect of roughness height (microposts) is shown by the data designated with the empty symbols in Fig. 2; everything else being the same, the presence of the microposts consistently enhances the LFP on all surfaces tested in this study but the magnitude of the enhancement is distinctively higher on the

nanoporous surface. As a result, the nanoporous surface with microposts can be consider an optimum (within the limits of our study), exhibiting the highest LFP at 453 °C, which is even beyond the critical point of water (374 °C) (Table I).[8]

Why do nanoporosity and microposts result in such a high LFP? High-speed imaging of the evaporating droplets shed light on the mechanisms, when we focused on the intermittent solid-liquid contacts in film boiling, as suggested by previous researches.[9] Actually, we observed thin liquid filaments intermittently connecting the droplet to the solid surface on the samples with microposts [Fig. 3(b)], whereas the filaments were not observed on the surfaces without microposts [Fig. 3(a)]. However, even in the presence of liquid filaments, the evaporation process was quite different depending on whether the surface was nanoporous or not. The gold and silicon oxide surfaces without nanoporosity stably sustained the liquid filaments, typically for a few milliseconds, without triggering any perturbation [Figs. 3(b) and 3(c)]. By contrast, the nanoporous surfaces instantaneously reacted to the filament contacts with violent splashes of tiny droplets around the large evaporating droplet [Fig. 3(d)]. This splashing severely disturbed the liquid-vapor interface and prevented the establishment of a stable vapor film at nominal surface temperatures as high as ∼453 °C.

Biance *et al.*[10] derived an analytical solution for the film thickness of a stationary evaporating droplet of radius, R, smaller than the capillary length, (R < a = $\sqrt{\sigma/\rho g}$), for a given surface superheat, ΔT,

$$e = C \left(\frac{k\Delta T \mu \rho g}{h_{fg}\rho_v \sigma^2} \right)^{1/3} R^{4/3}, \qquad (1)$$

where C, σ, k, μ, ρ, ρ_v, and h_{fg} are, respectively, an adjustable coefficient, surface tension, thermal conductivity, dynamic viscosity, density of liquid, density of vapor, and la-
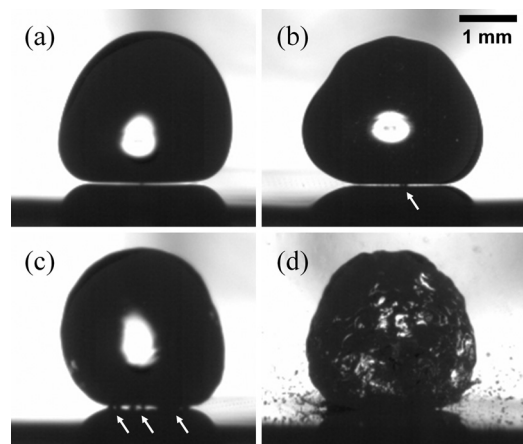

FIG. 3. Photographs of evaporating water droplets on test surfaces held at 400 °C: (a) Au without posts; (b) Au with 15 μm posts; (c) SiO$_2$ with 15 μm posts; (d) nanoporous SiO$_2$ layer with 15 μm posts. Arrows show location of droplet-to-surface bridging by liquid filaments.

tent heat of evaporation. For an evaporating droplet of 2R ∼ 2.9 mm on a surface of 400 °C (ΔT = 300 °C), the initial film thickness is estimated to be approximately 36 μm and then decreases monotonically as $R^{4/3}$. Thus, at 15 μm height, the microposts can initiate solid-liquid contacts, as shown in Fig. 3.

Once the liquid filaments are established, heterogeneous nucleation of bubbles can occur at the contact points, if there are cavities available for nucleation. Bernardin and Mudawar's[11] heterogeneous nucleation model of the LFP focuses on the surface superheat temperature required to initiate the growth of hemispherical vapor bubbles from the pre-existing surface cavities. The nanosized pores act as cavities for heterogeneous nucleation of bubbles. The pressure drop across a spherical bubble interface of radius r can be estimated using Young–Laplace equation as

$$P_g - P_f = \frac{2\sigma}{r}. \tag{2}$$

In combination with the Clausius–Clapeyron equation, Eq. (2) gives the following expression for the temperature required to initiate the nucleation of a hemispherical vapor bubble,[11]

$$T_{nucl} = T_{sat} \exp\left(\frac{2\sigma v_{fg}}{r h_{fg}}\right). \tag{3}$$

There exists a large difference in temperature for heterogeneous nucleation of bubbles between the nanoporous and nonporous surfaces, i.e., $T_{nanoporous} \sim 218$ °C versus $T_{nonporous} \sim 336$ °C, where nucleation diameter of 23 nm and 1 nm were assumed, respectively.[12,13] Therefore, bubbles more easily nucleate on the nanoporous surface and very rapidly grow in the highly superheated liquid. Starting from the Rayleigh equation for the inertia-controlled phase of bubble growth, it can be shown that $\Delta P \sim \rho V^2$, where V is the velocity of the expanding vapor interface and ΔP is the value of the pressure difference across the interface at the point of nucleation. For a bubble with a diameter of 23 nm, the estimated velocity, V, is of the order of 10 m/s. When the vapor phase velocity is greater than the critical velocity of Kenvin–Helmholtz instability, the liquid-vapor interface can

be disrupted. For the steam and water at atmospheric pressure, the critical velocity is approximately 8 m/s.[14] Therefore, the velocity of the expanding vapor interface for the 23 nm diameter bubble is fast enough to generate the splashes shown in Fig. 3(d). In this regard, it is concluded that nanoporosity (not solely high surface wettability) is an essential feature to enhance the LFP, and such enhancement occurs via prevention of the stable vapor film establishment, caused by heterogeneous nucleation of bubbles. The microposts on the surface intensify such effects by promoting intermittent liquid-surface contacts.

[1]H. Kim, G. DeWitt, T. McKrell, J. Buongiorno, and L.-W. Hu, Int. J. Multiphase Flow **35**, 427 (2009).
[2]H. Kim, J. Buongiorno, L.-W. Hu, and T. McKrell, Int. J. Heat Mass Transfer **53**, 1542 (2010).
[3]P. J. Berenson, J. Heat Transfer **83**, 351 (1961).
[4]R. E. Henry, AIChE Symp. Ser. **70**, 81 (1974).
[5]D. Lee, M. F. Rubner, and R. E. Cohen, Nano Lett. **6**, 2305 (2006).
[6]R. N. Wenzel, Ind. Eng. Chem. **28**, 988 (1936).
[7]S. C. Yao and K. Y. Cai, Exp. Therm. Fluid Sci. **1**, 363 (1988).
[8]The reported value of LFP is the nominal temperature of the test surface. Obviously, the local temperature at which the liquid-solid contact occurs must be below the critical point.
[9]W. S. Bradfield, Ind. Eng. Chem. Fundam. **5**, 200 (1966).
[10]A.-L. Biance, C. Clanet, and D. Quere, Phys. Fluids **15**, 1632 (2003).
[11]J. D. Bernardin and I. Mudawar, J. Heat Transfer **124**, 864 (2002).
[12]Note that these values of nucleation superheat are much higher than those normally encountered on engineering surfaces where *microcavities* are present.
[13]The calculated value of the heterogeneous nucleation temperature at d = 1 nm is higher than the homogeneous nucleation temperature (∼300 °C for water at atmospheric pressure) because the size of the vapor embryos responsible for homogeneous nucleation is of the order of a few nanometers. Therefore, the fluid nucleates homogeneously before it does so heterogeneously.
[14]V. P. Carey, *Liquid-Vapor Phase-Change Phenomena*, 2nd ed. (Taylor & Francis, New York, 2008), pp. 112–121.